

UNCLASSIFIED

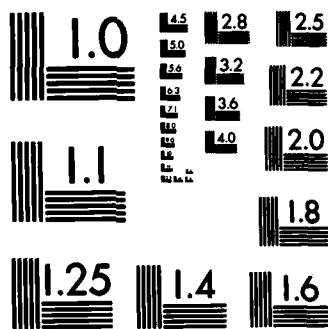
JUL 82 UM-016968-3 AFOSR-TR-82-1026

NL

END

Est. SEC:

530



REPORT DOCUMENTATION PAGE		READ INSTRUCTIONS BEFORE COMPLETING FORM
1. REPORT NUMBER <b>AFOSR-TR- 82 - 1026</b>	2. GOVT ACCESSION NO. <b>A122 296</b>	3. RECIPIENT'S CATALOG NUMBER
4. TITLE (and Subtitle) <b>DETONATION CHARACTERISTICS OF SOME DUSTS AND LIQUID-DUST SUSPENSIONS</b>		5. TYPE OF REPORT & PERIOD COVERED <b>ANNUAL 1 March 1981 - 1 May 1982</b>
6. AUTHOR(s) <b>C W KAUFFMAN P LEE J A NICHOLLS K WOOD M SICHEL</b>		6. PERFORMING ORG. REPORT NUMBER <b>UM 016968-3</b>
7. PERFORMING ORGANIZATION NAME AND ADDRESS <b>THE UNIVERSITY OF MICHIGAN DEPT OF AEROSPACE ENGINEERING ANN ARBOR, MI 48109</b>		8. CONTRACT OR GRANT NUMBER(s) <b>AFOSR 79-0093</b>
9. CONTROLLING OFFICE NAME AND ADDRESS <b>AIR FORCE OFFICE OF SCIENTIFIC RESEARCH/NA BOLLING AIR FORCE BASE, DC 20332</b>		10. PROGRAM ELEMENT PROJECT, TASK AREA & WORK UNIT NUMBERS <b>61102F 2308/A2</b>
11. MONITORING AGENCY NAME & ADDRESS (if different from Controlling Office)		12. REPORT DATE <b>July 1982</b>
		13. NUMBER OF PAGES <b>19</b>
		14. SECURITY CLASS. (of this report) <b>UNCLASSIFIED</b>
		15a. DECLASSIFICATION/DOWNGRADING SCHEDULE

DISTRIBUTION STATEMENT (of this Report)

Approved for Public Release; Distribution Unlimited

DISTRIBUTION STATEMENT (of the abstract entered in Block 20, if different from Report)

1. SUPPLEMENTARY NOTES

2. KEY WORDS (Continue on reverse side if necessary and identify by block number)

**MULTIPHASE DETONATIONS  
DUST EXPLOSIONS  
DETONATION INITIATION ENERGY**

20. ABSTRACT (Continue on reverse side if necessary and identify by block number)

This report presents the progress made in the last year on our study of the detonation properties of high explosive dusts when dispersed in air and suspended in liquids. The experimental facility is a modified form of a shock tube wherein the dust is blown through the tube and then a strong shock wave is transmitted into the heterogeneous mixture. Changes made to the facility in the past year are described. Two sizes of RDX particles were used; RDX-E (about 10  $\mu$ m) and RDX-A (about 150  $\mu$ m). Detonation was never obtained with the small RDX particles. Detonation was achieved with the larger RDX particles

AD A122296

FILE COPY

DEC 13 1982

A

p.3

UNCLASSIFIED

SECURITY CLASSIFICATION OF THIS PAGE(When Data Entered)

but only with some oxygen enrichment. Accordingly, many tests were conducted in air wherein various amounts of the oxidizer dust, ammonium perchlorate, were mixed in with the RDX dust. Again detonation was realized only with the large particles. Higher pressure ratios were measured than in the case of RDX-A and O<sub>2</sub> enriched air. In recognition of the importance of ignition time delay and reaction zone length to the initiation and propagation of detonation, some experiments were then conducted on the shock wave ignition of a fuel droplet (decane) containing the 10  $\mu$ m RDX particles. Shock waves of Mach number 3.5 were passed over a single drop in an O<sub>2</sub> atmosphere of ambient pressure and temperature. Significantly lower ignition delay times were measured when RDX was added to the decane. A range of conditions remains to be explored. Analytical studies have been in progress which closely relate to the experiments. The two phase relaxation zone behind the lead shock wave, including particle heating and reaction, continues to be modeled theoretically and some numerical calculations have been made.

Recommendation For	
CLASSIFICATION	<input checked="" type="checkbox"/>
EXCLUDED	<input type="checkbox"/>
EXCLUDED	<input type="checkbox"/>
EXCLUDED	<input type="checkbox"/>



Distribution/	
Availability Codes	
Avail and/or	Special
A	

Pg. 2

UNCLASSIFIED

SECURITY CLASSIFICATION OF THIS PAGE(When Data Entered)

## RESEARCH OBJECTIVES

AFOSR-79-0093

✓ The main objective of this research is to determine the detonation characteristics of dusts when dispersed in air under unconfined conditions. Important factors which bear on this problem, and hence which would be investigated, include the properties of the dust, the concentration of the dust, the size of the dust particles, the effects of excess oxygen, the energy of the initiating source, and the structure of the reaction zone. For a range of conditions, then, it is desirable to determine the pressure history within and behind the reaction zone, the wave velocity, the ignition time delay of the particles behind the leading shock wave, and to obtain high speed streak and framing photographs of the wave and reaction zone. The experimental results would be utilized in connection with an analytical treatment to develop a model for the initiation of such detonations. An interesting ramification of this research is the "three-phase" detonation. That is, the detonability aspects of dust particles entrained in liquid fuel droplets. ←

## STATUS OF THE RESEARCH EFFORT

The experimental facility developed for these studies and the experimental and analytical results obtained were presented in last year's annual report<sup>1</sup>. In this report a small part of that report is repeated for the sake of continuity but the emphasis is on alterations to the facility and the research results obtained in this past year.

AIR FORCE OFFICE OF SCIENTIFIC RESEARCH (AFOSR)  
NOTICE OF INFORMATION TO DTIC  
This technical report has been reviewed and is  
approved for public release IAW AFR 190-12.  
Distribution is unlimited.  
MATTHEW J. KAMMER  
Chief, Technical Information Division

Approved for public release;  
distribution unlimited.

### Experimental Facility

The main parts of the horizontal shock tube facility are shown in Fig. 1. The driver section consists of a 5 ft length of heavy wall 3 in. ID circular tubing with volume spacers (used to give different driver volumes) inside. During the past months, it was found necessary to refit the driver section due to the very high pressure (3500 psi) of helium gas being used for droplet ignition tests. These high pressures caused the spacers to become dislodged by overloading the support pipe during the shock release. The refitting required a heavier pipe to be used to hold the spacers in place under these heavy load conditions (see Fig. 2). For detonation tests with the suspended dust, the driver was charged with a hydrogen-helium-oxygen ( $2\text{H}_2 + \text{O}_2 + 1.5 \text{ He}$ ) mixture. The mixture was initiated by a glow plug which resulted in a blast wave being transmitted through the transition section and into the test (driven) section. The transition and driver sections were separated by a Mylar diaphragm which ruptured when struck by the detonation wave from the driver. Three functions were performed in the transition section of the shock tube. In this section, the dust was introduced from the feeder in a downstream direction by means of a carrier gas flow. Another gas flow was introduced in this section to be used as an oxidizer. The transition section also adapts the circular driver to the rectangular test section and there is an area reduction of 47%.

The feeder was able to withstand the pressures of a dust and gaseous oxidizer detonation but not the increased pressure caused by using the solid oxidizer ammonium perchlorate ( $\text{NH}_4\text{ClO}_4$ ). The feeder was destroyed by an explosion during an RDX-AP run. A new feeder was designed and built and has been used successfully for the past six months. This new design is of

a heavier construction and has a greater number of induced airflow nozzles, from five to seven, as shown in Fig. 3. The new feeder is able to accommodate a dust feeding rate three times that of the original feeder allowing higher reactive dust loadings in the driven section.

The test section is a 20 ft long rectangular stainless steel tube of internal dimensions 1.5 x 2.5 in. The instrumentation is shown in Fig. 1 and consists of six pressure switches and four pressure transducers (the 4th one was added during the year). A photocell was also used and was installed at the same location as the third pressure transducer. This allowed the measurement of the delay time between the shock and flame front. In Fig. 4, typical pressure and light traces are shown for detonation and non-detonation tests. The pressure rises are higher, and remain high, and the ignition delay is shorter for the detonation run.

In order to observe the details of the interaction between the incident waves and the particles, an optical section was installed, as shown in Fig. 1. The windows of this section are of schlieren quality glass. This system was used for high speed drum camera records of dust detonations and for the shock wave ignition studies of RDX-liquid fuel drops.

Outside of a few runs with grain dust, the dust used to date has been RDX, lightly coated with a plastic. Two sizes have been used, RDX-A (nominally 150  $\mu\text{m}$ ) and RDX-E (nominally 10  $\mu\text{m}$ ).

### Experimental Results

Previously, experimental runs were made to detonate RDX-A and RDX-E dusts convected in gases. The only detonation experienced was RDX-A, the larger particle size, in oxygen enriched air (12%  $\text{O}_2$ , 88% air) with an equivalence ratio of  $\phi = .94$ . In this situation the RDX loading

density was  $1300 \text{ gms/m}^3$ . The Mach number and pressure ratio at the tube exit were 5.1 and 28 respectively. RDX-A did not detonate with pure air and RDX-E did not detonate with pure air or the 12%  $\text{O}_2$  plus 88% air mixture. Neither of the RDX sizes detonated with pure  $\text{N}_2$ , although ignition did occur. Figure 5 shows the comparison of time-distance trajectories of detonation and non-detonation runs. The detonation maintains a constant velocity.

At that point it was deemed of interest to investigate the oxygen enrichment, which is evidently needed, through use of a solid oxidizer dust. Accordingly, further tests were made with the use of AP, ammonium perchlorate ( $\text{NH}_4\text{ClO}_4$ ), mixed with the RDX dust. Theoretical calculations indicated that such mixtures in air could lead to very high pressures<sup>1</sup>. The amount of AP added was such that the oxidizer consisted of 20% AP and 80% air on a mass basis. The amount of RDX is denoted by the equivalence ratio,  $\phi$ , as defined by the computer program of Gordon and McBride<sup>2</sup>. The equivalence ratio versus RDX concentration for various fractions of AP in the oxidizer is shown in Fig. 6. At higher dust densities (above  $500 \text{ gm/m}^3$ ), the AP plays the role of oxidizer, therefore the larger the fraction of AP the lower the equivalence ratio. However, at lower RDX densities, AP behaves more as a fuel than oxidizer, therefore the larger the fraction of AP the higher the equivalence ratio. This is theoretically verified according to the NASA Gordon-McBride computer program<sup>2</sup>. The computer output for the products of reaction showed that at low dust densities a mild increase of AP would result in a significant increase of the products such as  $\text{ClO}$ ,  $\text{H}_2\text{O}$  and  $\text{NO}$ . In the AP-RDX runs, a small amount of Cabosil  $\text{Al}_2\text{O}_3$  was added to the dust to improve the dispersion characteristics of the dust along the tube. At  $\phi = .94$ , detonation



was not observed with the RDX-A-AP-Cabosil dust convected in air, whereas a detonation was achieved with RDX-A in an oxygen enriched airflow at the same equivalence ratio (Fig. 7). This probably should not be surprising in that the oxygen in the AP is not as available for reaction as gaseous oxygen. However, at lower equivalence ratios, the RDX-A-AP-Cabosil dust eventually established detonation at  $\phi = .88$  and  $\phi = .84$ . The Mach number and pressure ratio near the end of the tube were approximately 5.0 and 34 for  $\phi = .88$ , and approximately 4.9 and 32 for  $\phi = .84$  (Fig. 8). The pressure ratios of the RDX-A/AP mixture are higher than that of the RDX-A dust only when in an oxygen air mixture. Similar experimental runs were also made with RDX-E, the smaller particles, mixed with AP and Cabosil. Several equivalence ratios were tested at various initiator energies but no detonation was observed with the RDX-E/AP dust.

For the RDX-A-AP-Cabosil mixtures operating at a constant driver pressure of 119.3 psia, the exit Mach numbers and pressure ratios were 5.3 and 40 for  $\phi = 1.1$ , 5.2 and 38 for  $\phi = 1.0$ , and 5.0 and 37 for  $\phi = .9$ , respectively. These pressure ratios are high compared to RDX runs without the AP. Figure 9 shows the decay of the waves using RDX-A and AP,  $\phi = 1.0$ , for three different initiator energies. The larger initiation energies give stronger waves throughout, of course. The lowest energy run appears to be definitely decaying throughout. It is not clear with the two higher energies; there is some indication that they may be transitioning to detonation.

Streak schlieren photographs were taken to investigate the dust detonation processes. Figure 10 shows the wave propagating through an RDX-A cloud. The leading shock is indicated by the first sharp slanting line crossing the photograph. The particle path can be observed immediately behind the shock wave, accelerating to the right in the shocked gas

flow direction. Further behind the shock, where the particle traces start to disappear, is presumably the beginning of the reaction zone. The ignition delay, defined as the time elapsed between the leading shock and the beginning of the reaction zone, is about 45  $\mu$ sec.

Another phase of the research involves the detonation characteristics of RDX dust entrained in liquid fuel drops. This might be referred to as three phase detonation. The initial studies have concentrated on the shock wave ignition of an individual drop. As indicated earlier, the detonation tube was modified so as to serve as a regular shock tube. High pressure helium was used in the driver section. Individual decane drops with RDX-E (small particles) mixed in were suspended from a needle in the test section. Streak schlieren photographs were obtained to investigate the ignition characteristics of the droplets. The streak photographs in Fig. 11 show a comparison between a decane drop with and without RDX. Figure 11a is a decane droplet alone whereas Fig. 11b is a RDX-decane droplet consisting of 40/60 (by weight) mixture of RDX-E and decane. Both droplets contain Cabosil (5% of the weight of decane) which increases, for both droplets, the viscosity and surface tension. Each droplet is 3000  $\mu$ m in diameter and exposed to a shock with  $M = 3.5$  in one atmosphere of pure oxygen. Both photographs show similar structures. The aerodynamic forces on the droplet behind the shock causes the drop to breakup. Following the breakup, the wake (indicated by the growth of the dark region) is formed behind the drop. The acceleration of the disintegrating droplet in the shocked gas flow is indicated by the curvature of the droplet's leading edge trajectory. A bow shock is formed in front of the leading edge. After a delay of  $T_{ig}$ , ignition (indicated by the bright burst of flame) occurs in the wake region and the "flame" propagates very rapidly upstream toward the leading edge of the drop.

The ignition delay,  $T_{ig}$ , and the "flame" speed are estimated to be 85  $\mu$ sec and 1700 m/sec for the RDX-decane droplet and 130  $\mu$ sec and 1400 m/sec for the decane droplet. These high "flame" speeds indicate that they are really blast waves driven by combustion. The ignition delays are relatively long as compared to most heterogeneous detonations. However, the shock Mach number of 3.5 is low compared to most detonation Mach numbers and, in the latter case, the delays would be much shorter. It is very interesting that the ignition delay is appreciably lower for the drop with the RDX.

The stagnation temperature behind the bow shock is 1300°K for an incident shock of  $M = 3.5$ . It appears that this high temperature causes some chemical reaction at the leading edge of the drop just behind the bow shock. This luminosity, observable in both photographs, is less distinct than the main ignition in the wake region. The incident shock strength, the oxidizer, and the composition and size of the droplets are expected to have distinct effects on these droplet ignition characteristics. Further work is in progress to study the ignition characteristics at various conditions.

#### Analytical Results

The induction zone between the leading shock wave and the start of significant combustion heat release has an important influence on the detonability of dusts. In this region the dust particles are suddenly exposed to the supersonic flow induced by the shock wave. As a result the particles are convectively heated and accelerated so that the relative velocity between the particles and the gas decreases. At the same time the interaction between the gas and particle flows will result in an increase in the gas temperature and pressure.

To deal with particle ignition delay it therefore is essential to consider the two phase flow behind the leading shock front.<sup>1</sup> The equations describing such flows are presented in detail by Rudinger<sup>3</sup> and have been used to compute the conditions in the induction zone of dust detonations. For steady flow the gas and particle conservation equations reduce to a system of algebraic equations plus two differential equations for particle motion and heating. The Nusselt number and the drag coefficient are important empirical inputs to these calculations.

A computer code for solving these equations has been developed which makes it possible to study the behavior of the relaxation zone over a wide range of conditions. A typical output showing the dimensionless gas and particle temperatures,  $TN$  and  $TPN$ , and the dimensionless gas and particle velocities,  $UN$  and  $UPN$ , behind a Mach 1.5 shock wave moving through a cloud of 10  $\mu m$  glass spheres in air is shown in Figs. 12 and 13. The air sound speed and temperature ahead of the shock are used as reference quantities and the ratio of particle to gas mass flow has a value of 0.2. The variation of temperature and velocity is shown as a function both of distance and time respectively in Figs. 12 and 13. In this particular example, relaxation is almost complete after 200  $\mu sec$ . The empirical expressions used for the drag coefficient and the Nusselt number are given in Fig. 12.

These results are not, in themselves, new; however, the capability of computing the shock relaxation zone structure over a wide range of conditions is an essential first step to studying the induction process. The behavior of the structure for small and larger particles may help explain why RDX dusts with smaller particles are more difficult to detonate.

The behavior of the relaxation zone must be coupled to the heating and reaction of the individual particles. The results shown above assume uniform particle temperature and do not account for chemical reactions. Analysis of individual particle heating in which internal temperature variation and surface as well as internal heterogeneous reactions are taken into account has also been initiated. In essence this study involves the numerical solution of the unsteady heat conduction equation with source terms to account for reactive heating terms and boundary conditions which account for convective heating. Here again a numerical code which permits rapid parametric studies has been developed.

The relaxation and particle heating codes are now being applied to the study of dust-oxidizer mixtures corresponding to those which have been studied experimentally.

#### REFERENCES

1. "Detonation Characteristics of Dusts Dispersed in Air," C.W. Kauffman et al., AFOSR-TR-81-0595, UM 016968-2, Annual Report, Aerospace Engineering, The University of Michigan, May 1981.
2. Gordon, S. and McBride, B.J., "Computer Program for Calculation of Complex Chemical Equilibrium Compositions, Rocket Performance, Incident and Reflected Shocks, and Chapman-Jouguet Detonation," NASA-SP-273, 1971, Interim Revision, March 1976.
3. Rudinger, G., "Relaxation in Gas Particle Flow," Nonequilibrium Flows," Part I (P.P. Wegener, ed.), Marcel Dekker, NY, 1969.

#### PUBLICATIONS

1. Kauffman, C.W., Nicholls, J.A., "Dust Explosion Research at The University of Michigan," International Specialists Meeting on Fuel-Air Explosions, McGill University, Montreal, Canada, 1981; in forthcoming proceedings, University of Waterloo Press.
2. "The Static and Dynamic Impulse Generated by Two Phase Detonations," Phys. Fl. 25, 1982, 38-44.

#### PROFESSIONAL PERSONNEL

Professor J.A. Nicholls, Project Director  
Dr. C.W. Kauffman, Associate Research Scientist, Co-Principal Investigator  
Professor M. Sichel, Co-Principal Investigator  
P. Lee, Doctoral student  
K. Wood, Undergraduate

#### INTERACTIONS, NEW DISCOVERIES, OTHER STATEMENTS

A new phase of research was initiated during this period which could be referred to as three phase detonation. That is the liquid fuel drops have entrained small solid fuel particles and the oxidizer is gaseous. A critical aspect of such detonations is the reaction zone behind the lead shock wave. The experiments consisted of exposing a decane fuel drop, with and without entrained RDX dust, in oxygen to a Mach 3.5 shock wave. The ignition delay time was markedly reduced by the presence of the solid particles.

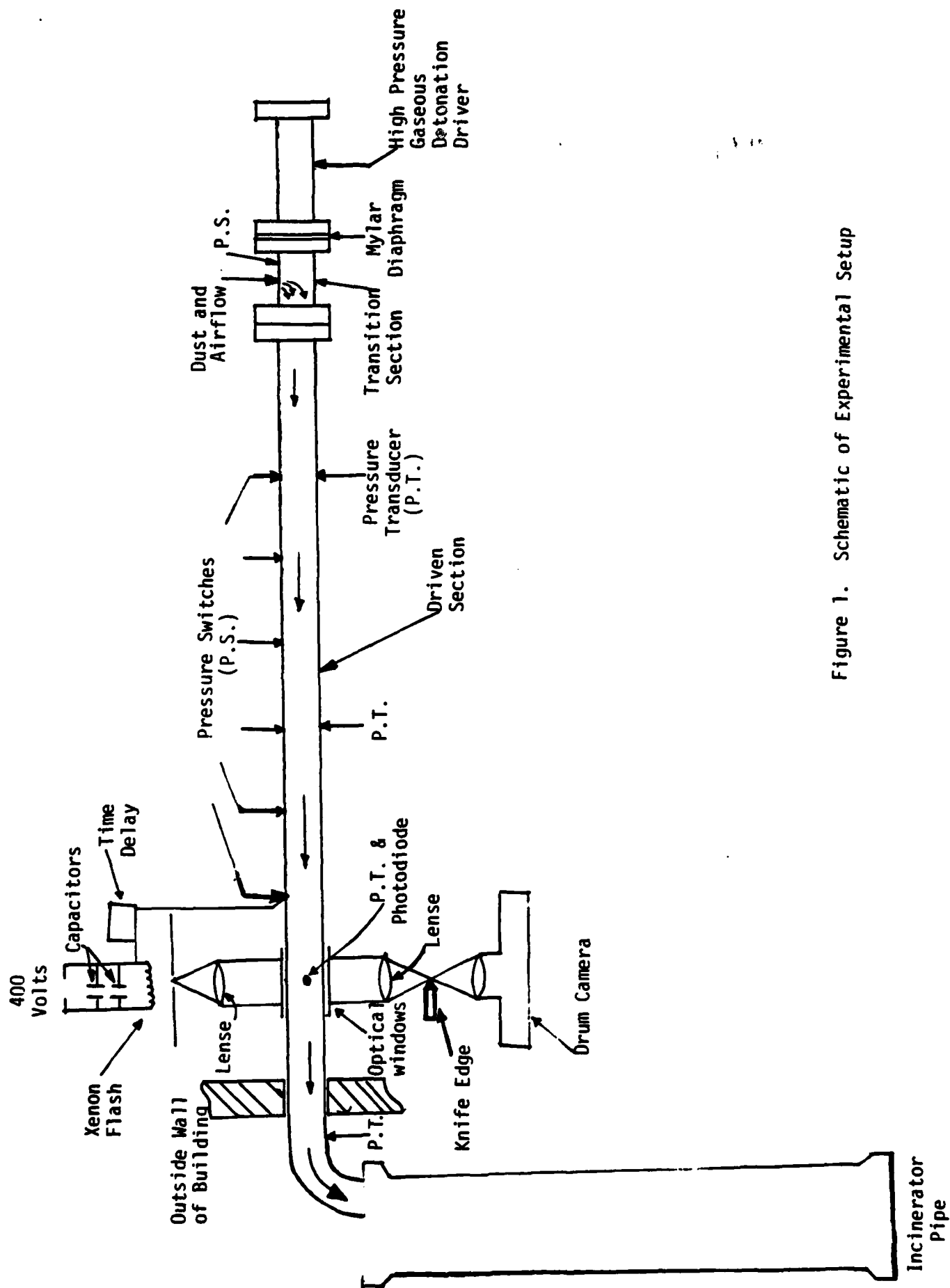


Figure 1. Schematic of Experimental Setup

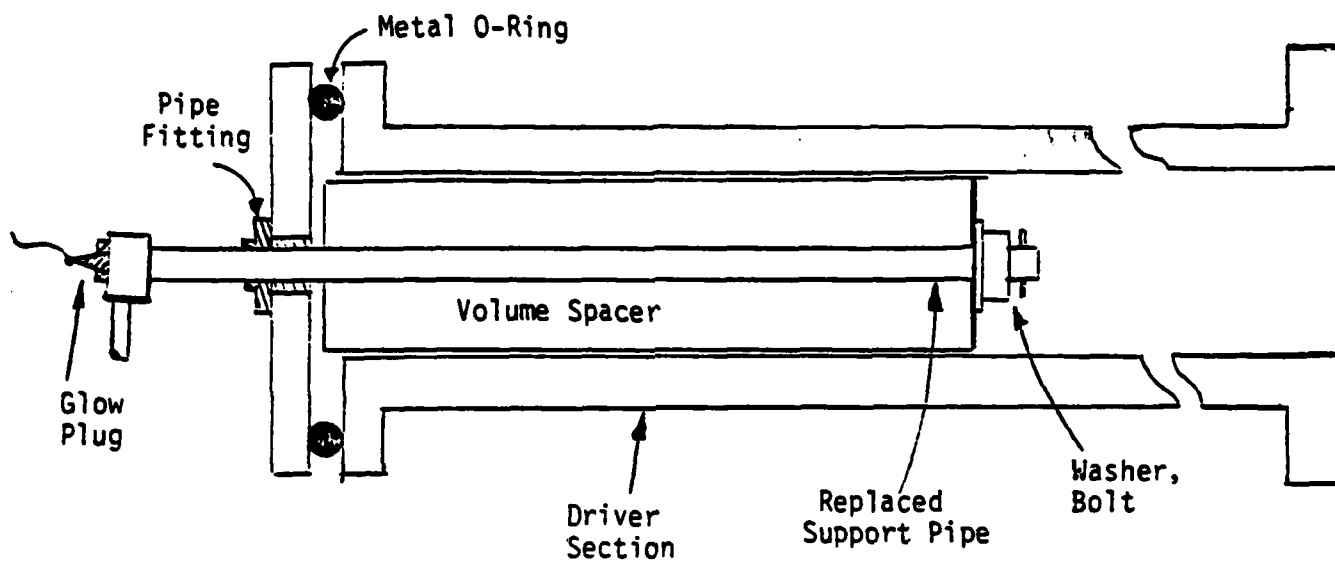


Figure 2. Driver Cross Section

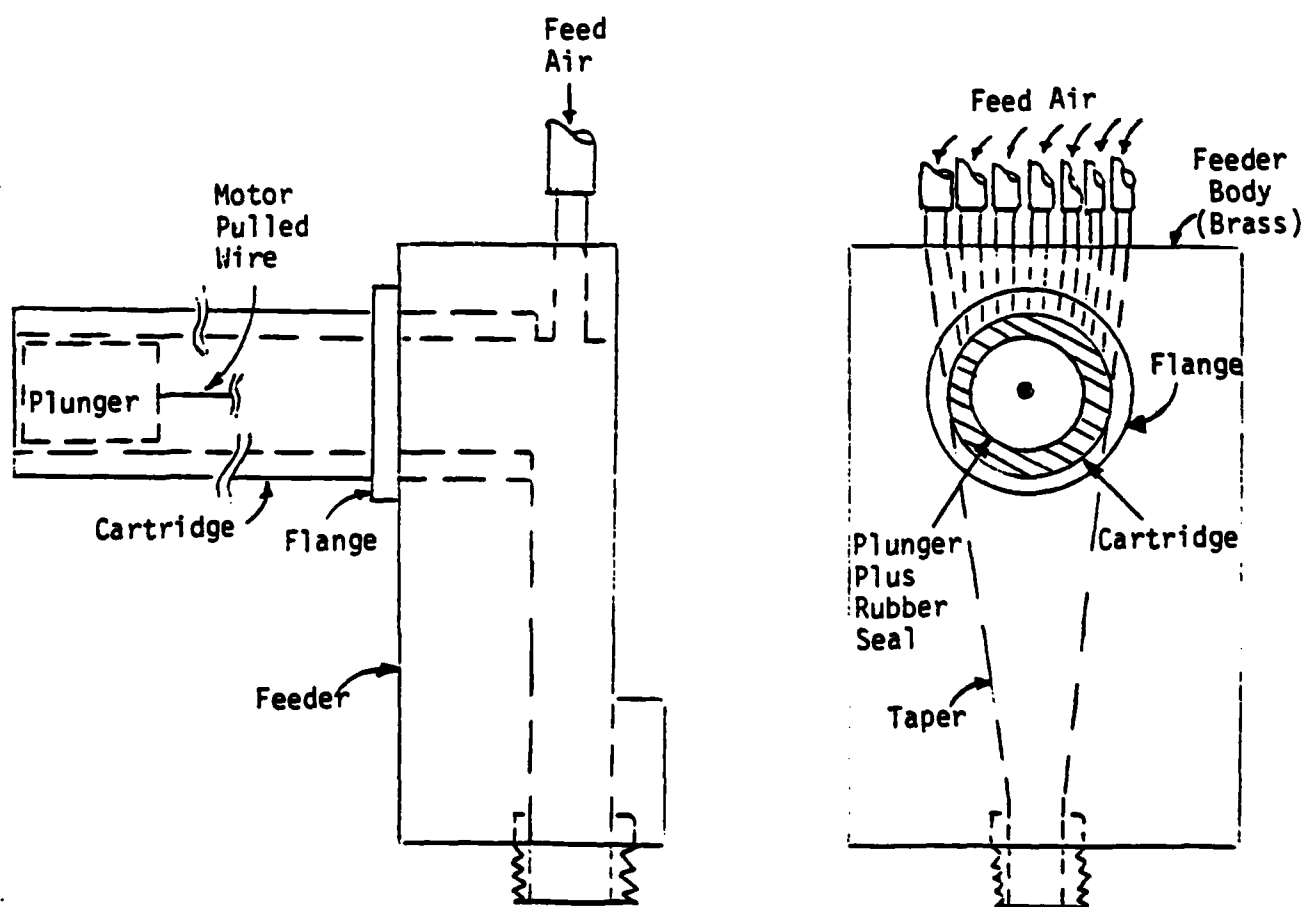


Figure 3. Feeder



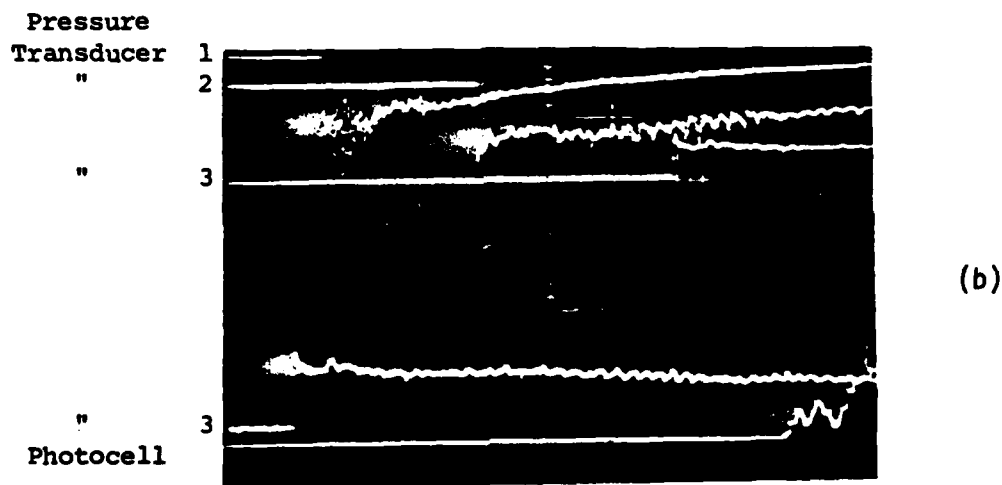
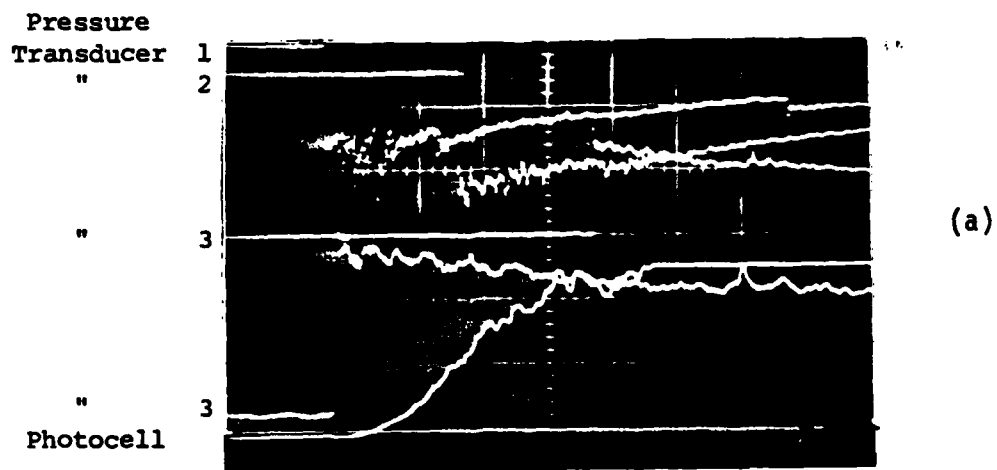


Figure 4. Light Emission and Pressure Records  
 Pressure Transducers 1, 2, and 3, respectively,  
 0.5 msec/div. Pressure Transducer 3 and the  
 Photocell at the same location, 0.1 msec/div.

a) Detonation, Run #259, RDXA 1300 gm/m<sup>3</sup>, 88% Air,  
 12% O<sub>2</sub>, Driver Pressure 119.3 psia, 1/4 Driver.

b) Non-detonation, Run #272, RDXA 1300 gm/m<sup>3</sup>, 100% N<sub>2</sub>,  
 Driver Pressure 119.3 psia, 1/4 Driver.

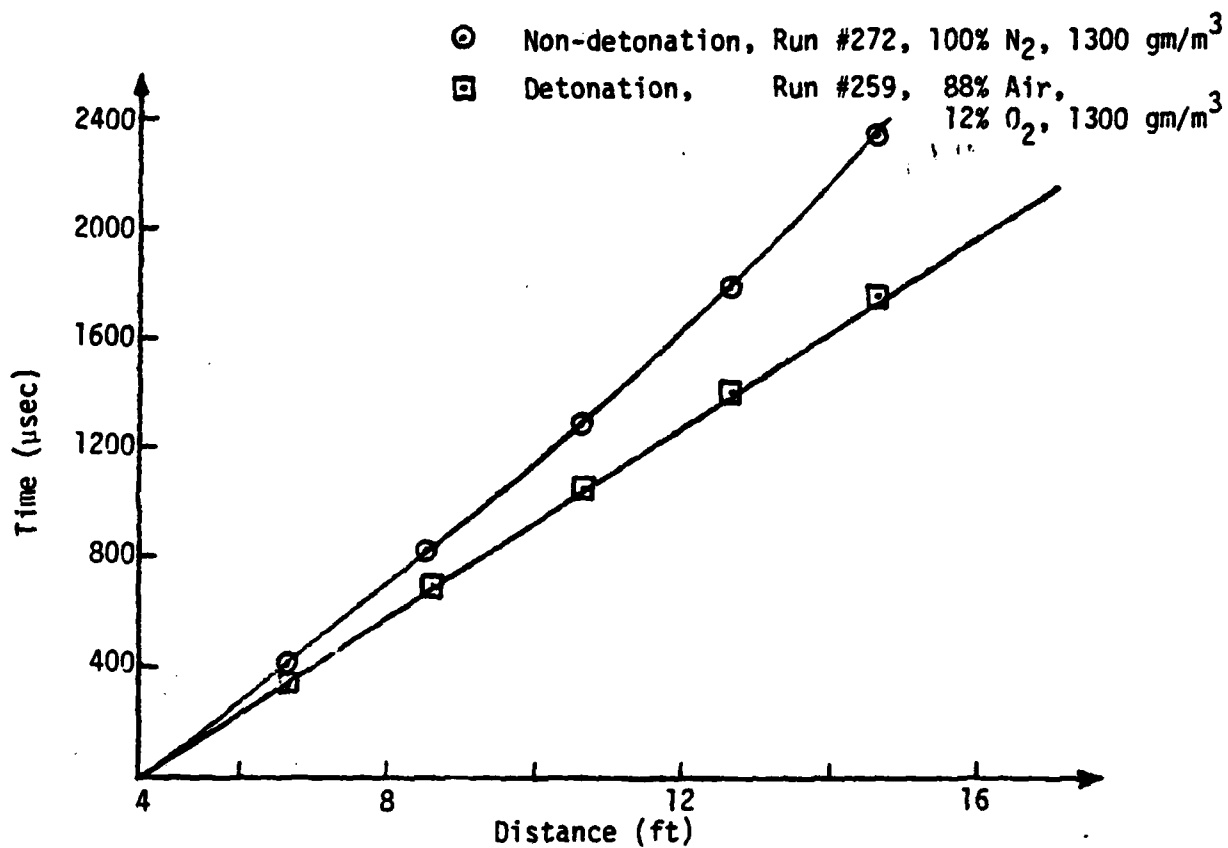


Figure 5. Variations of Wave Position Versus Time

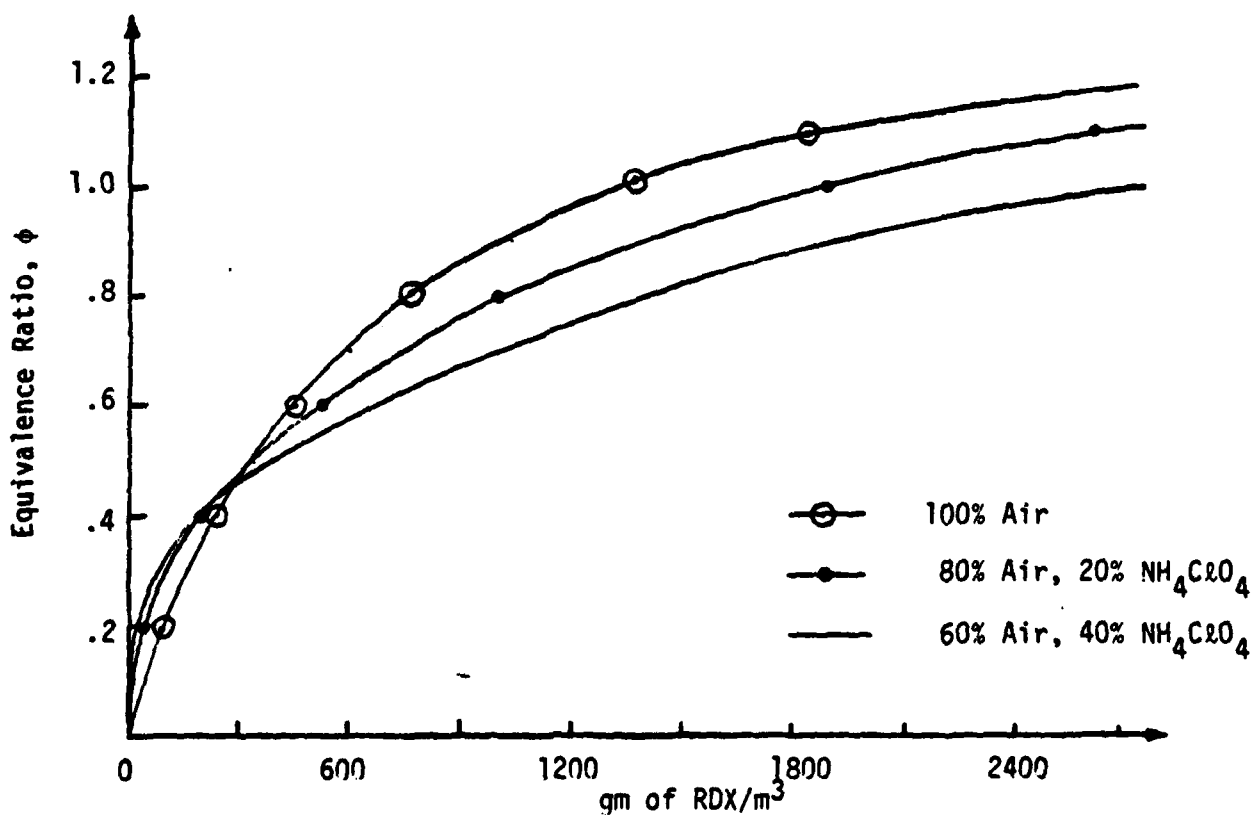


Figure 6. Dust Density Versus Equivalence Ratio

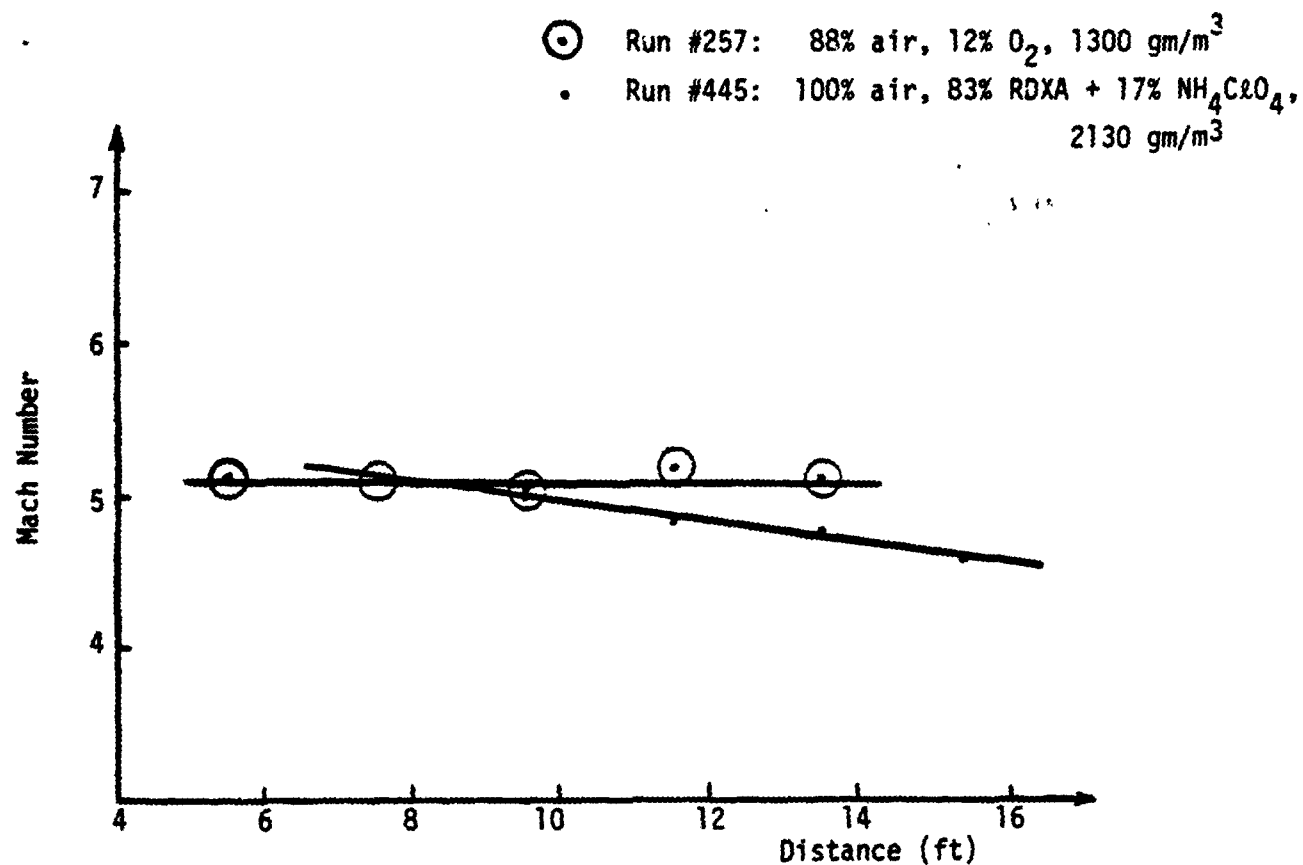


Figure 7. Wave Mach Number, RDX-A,  $\phi = .94$   
Driver Pressure, 119.3 psia, 1/4 Driver.

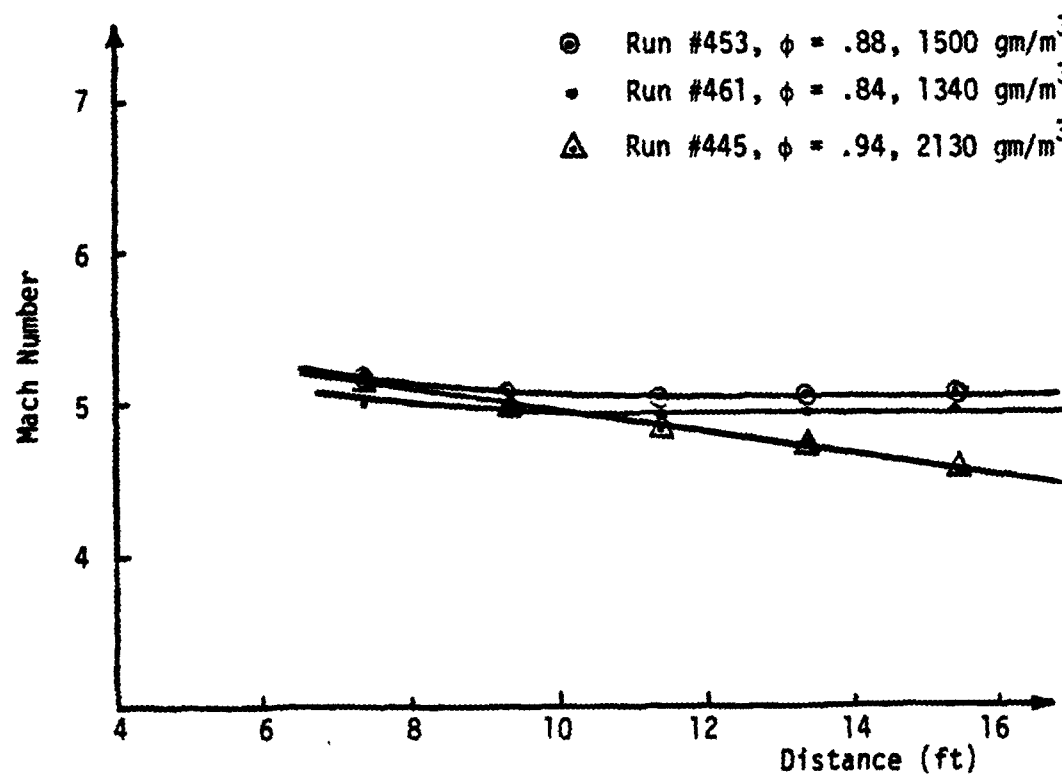


Figure 8. Wave Mach Number, 83% RDXA + 17% Ammonium Perchlorate  
100% Air, Driver Pressure 119.3 psia, 1/4 Driver.

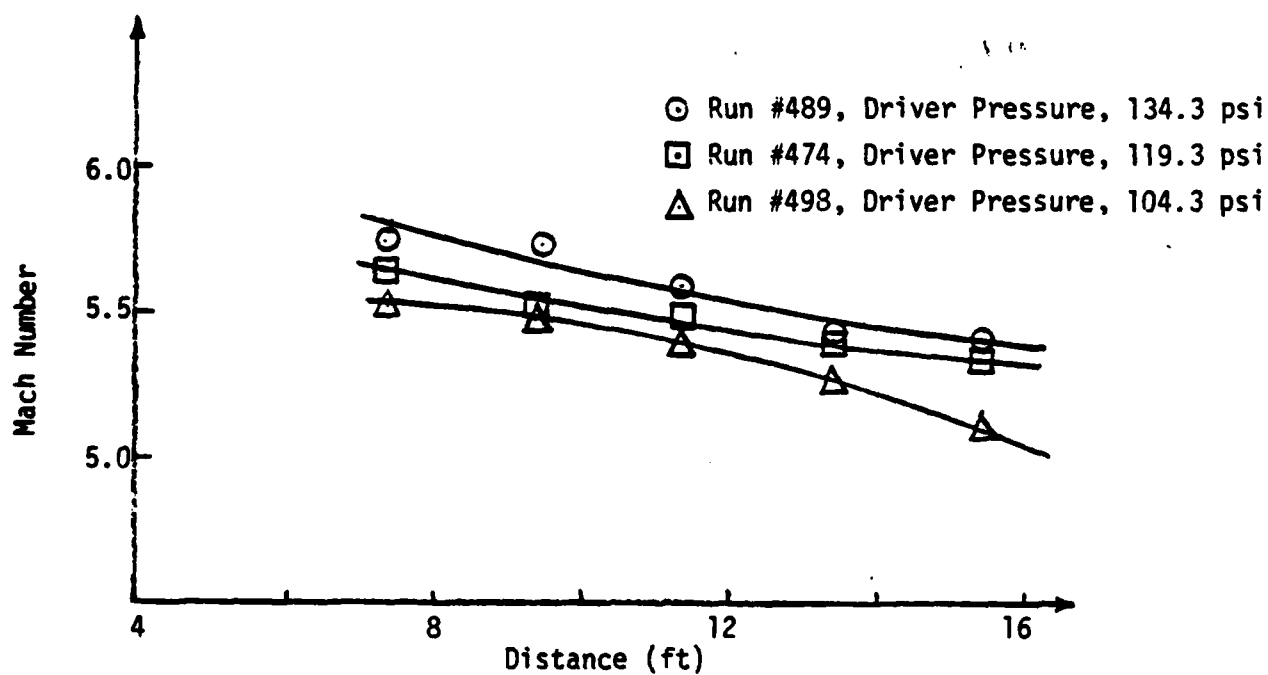


Figure 9. Wave Mach Number, 85% RDXA + 15% Ammonium Perchlorate, 100% Air, 1/4 Driver,  $\phi = 1.0$ .

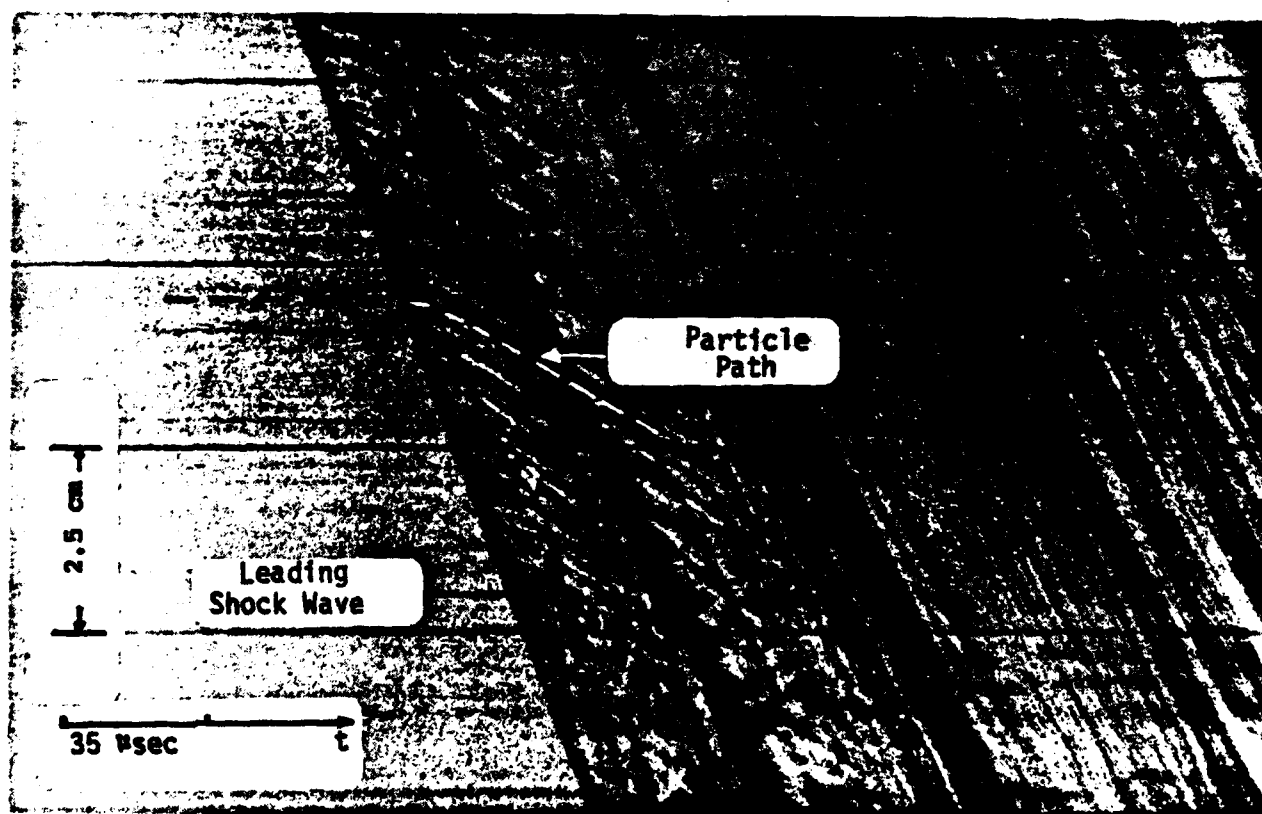


Figure 10. Run #386, RDXA/Air, 1300 gm/m<sup>3</sup>  
Driver Pressure, 119.3 psia, 1/4 Driver.

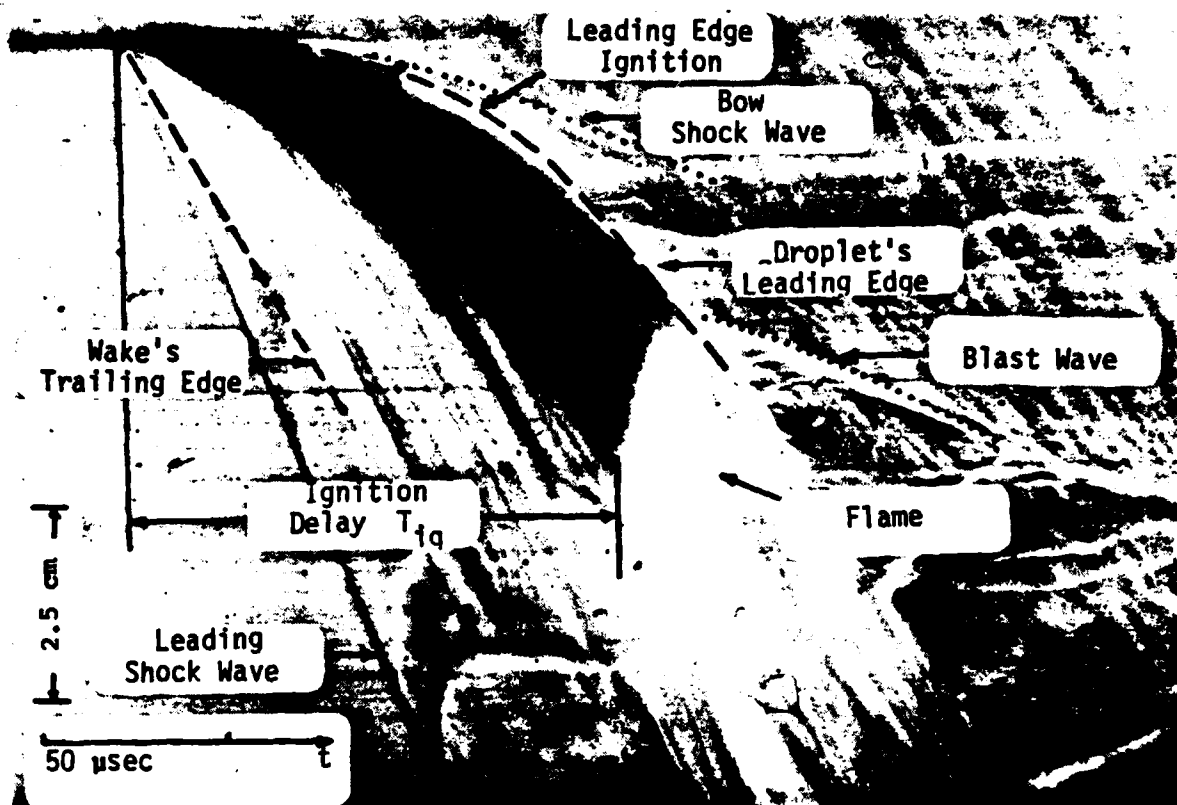


Figure 11(a). Run #501, Decane/Cabosil Droplet, 3000 μm,  $M = 3.5$ .

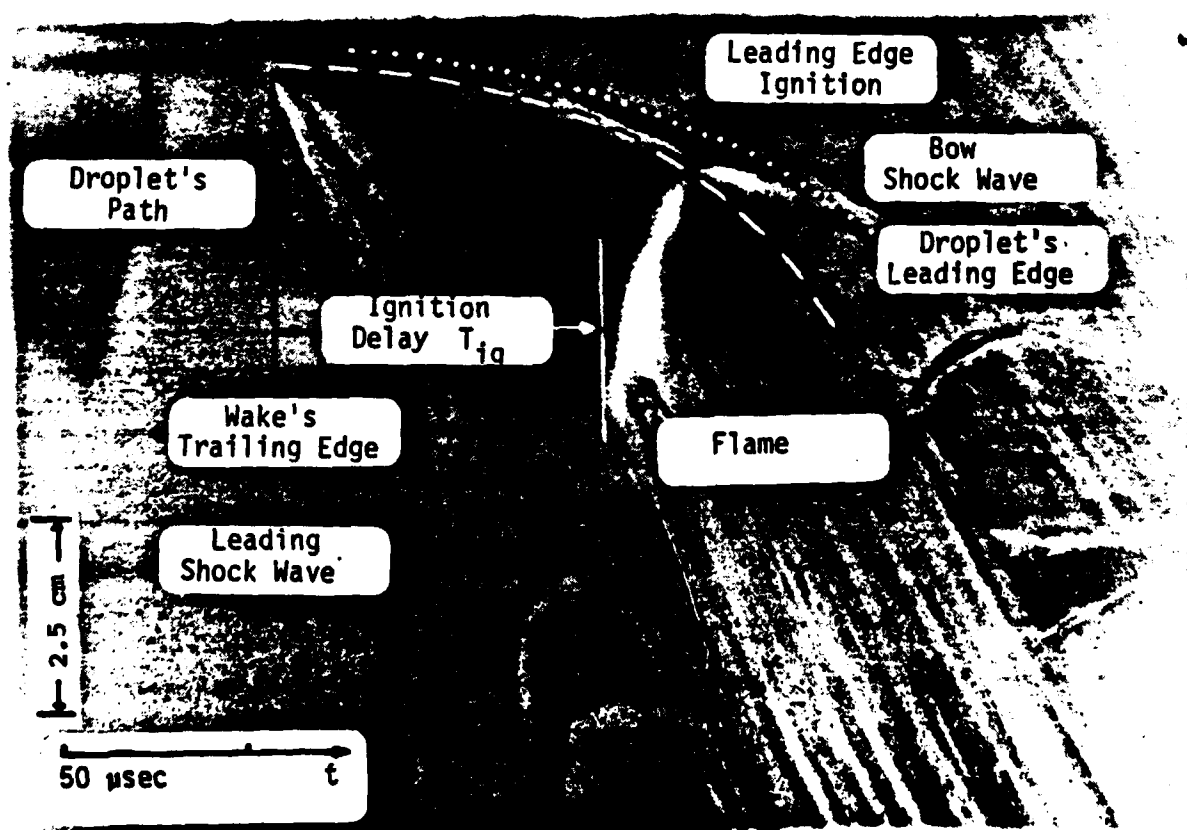


Figure 11(b). Run #502, RDX-E/Decane/Cabosil Droplet, 3000 μm,  $M = 3.5$ .

# RELAXATION ZONE BEHIND SHOCK WAVE

$$CD=24/RE+4/(RE**(1/3)) \quad NU=2+0.53(RE**(1/2))$$

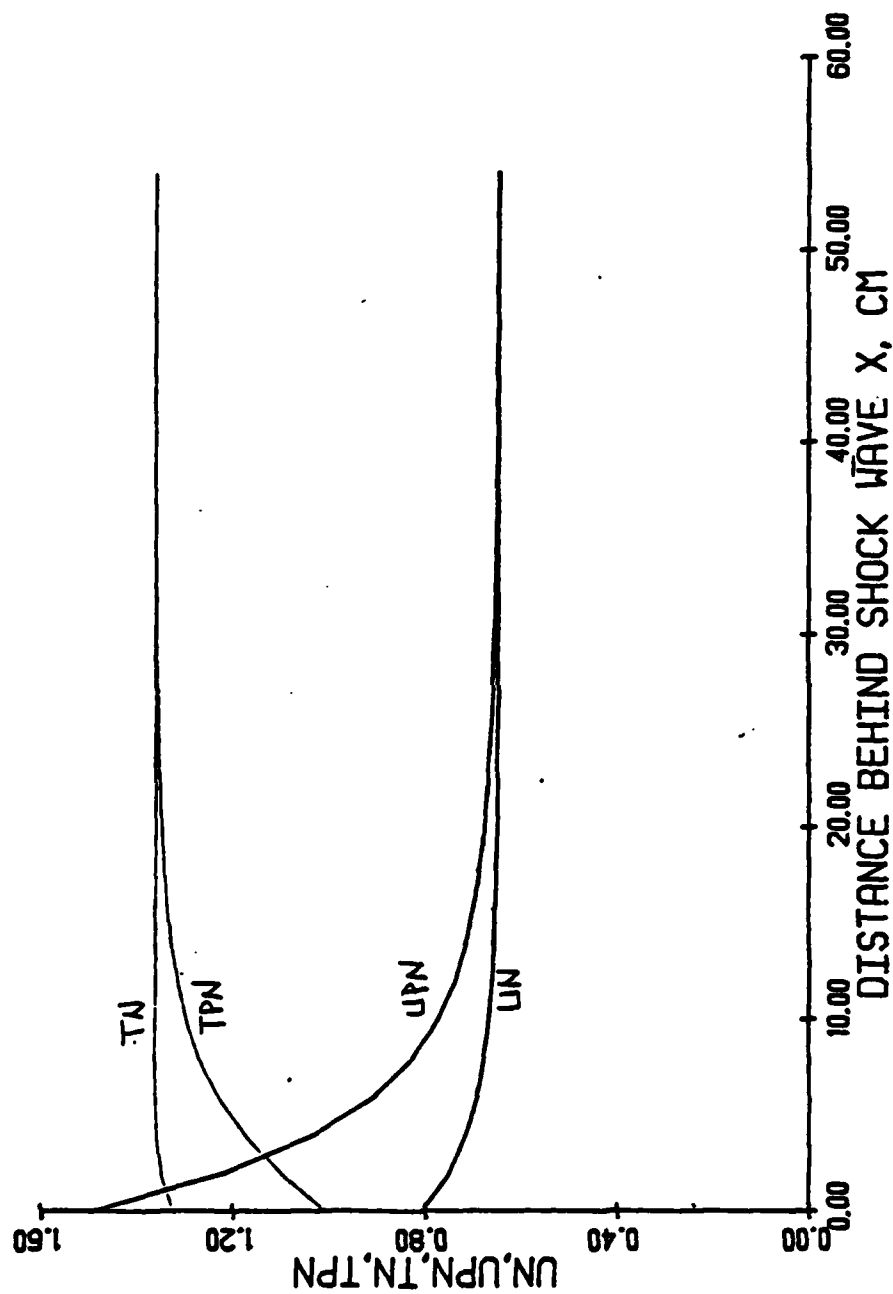


Figure 12. Variation of Gas and Particle Velocity and Temperature with Distance in the Shock Relaxation Zone.

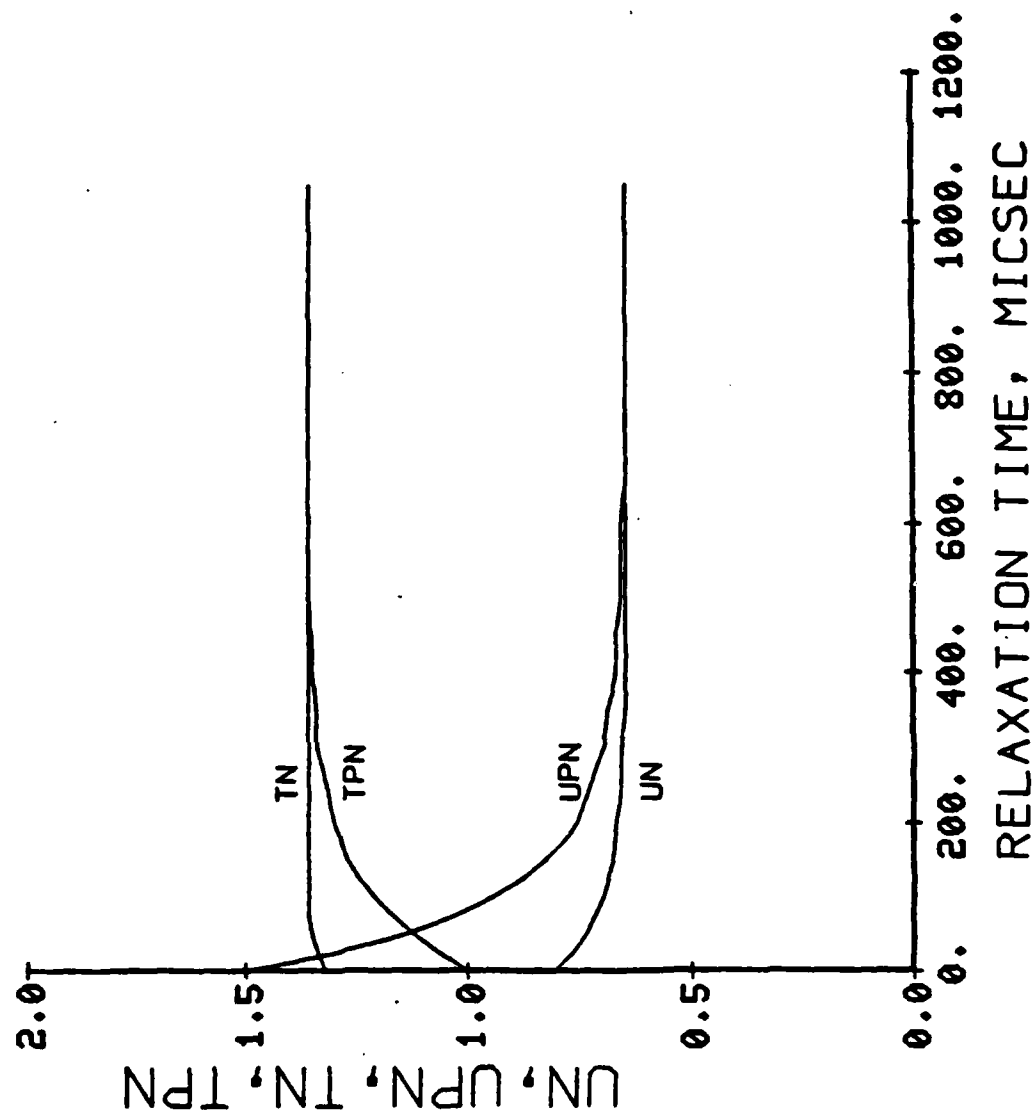


Figure 13. Variation of Gas and Particle Velocity and Temperature with Time in the Shock Relaxation Zone.